Embedding Meshes in Boolean Cubes by Graph Decomposition

Ching-Tien Ho and S. Lennart Johnsson

YALEU/DCS/TR-746
September 1989

To appear in the Journal of Parallel and Distributed Computing
as a special issue of "Algorithms, Hypercubes, Computers"
March 1990

Embedding Meshes in Boolean Cubes by Graph Decomposition

Ching-Tien Ho*
IBM Almaden Research Center
650 Harry Road
San Jose, CA 95120
Ho@ibm.com

S. Lennart Johnsson†
Departments of Computer Science
and Electrical Engineering,
Yale University
New Haven, CT 06520
Johnsson@cs.yale.edu, Johnsson@think.com

Abstract. This paper explores the embeddings of multidimensional meshes into minimal Boolean cubes by graph decomposition. The dilation and the congestion of the product graph $(G_1 \times G_2) \rightarrow (H_1 \times H_2)$ is the maximum of the dilation and congestion for the two embeddings $G_1 \rightarrow H_1$ and $G_2 \rightarrow H_2$. The graph decomposition technique can be used to improve the average dilation and average congestion. The graph decomposition technique combined with some particular two-dimensional embeddings allows for minimal-expansion, dilation-two, congestion-two embeddings of about 87% of all two-dimensional meshes, with a significantly lower average dilation and congestion than by modified line compression [4]. For three-dimensional meshes we show that the graph decomposition technique, together with two three-dimensional mesh embeddings presented in this paper and modified line compression, yields dilation-two embeddings of more than 96% of all three-dimensional meshes contained in a $512 \times 512 \times 512$ mesh. The graph decomposition technique is also used to generalize the mesh embeddings to meshes with wrap-around. The dilation increases by at most one compared to a mesh without wrap-around. The expansion is preserved for the majority of meshes, if a wrap-around feature is added to the mesh.

1 Introduction

Many linear algebra computations can be performed effectively on processor networks configured as two-dimensional meshes, with or without wrap-around. Processor networks configured as two- or higher dimensional meshes are also effective for the solution of partial differential equations whenever regular grids are appropriate. Though grid computations are frequently used, interconnection networks for parallel computers must be chosen to efficiently support many forms of communication. Boolean cube networks are currently used in several architectures. These networks are versatile in that they can emulate many other networks with little or no slowdown.

Embedding meshes in Boolean cubes by encoding the indices of each axis in a Gray code

*Most of the work was done while the author was with the Department of Computer Science, Yale University.

†The author is also with Thinking Machines Corp., 245 First Street, Cambridge, MA 02142. This work was supported in part by AFOSR-89-0382 and ONR Contract No. N00014-86-K-0310.

[20] yields a nearest neighbor embedding of adjacent nodes [14]. However, if the length of the axis is not a power of two, the Gray code embedding forces the number of processors allocated to an axis to be a power of two. For meshes of high dimension, this may yield a very poor processor utilization. Havel and Móravek [11] proved that any nearest-neighbor embedding must have the same processor utilization as that offered by the binary-reflected Gray code. Whenever the Gray code does not yield the maximum processor utilization, an increased utilization can only be achieved if some adjacent mesh nodes are assigned to Boolean cube nodes at a distance of at least two. The length of the path into which a mesh edge is mapped is the dilation of the edge, and the maximum dilation of any edge is the dilation of the embedding. The expansion of the embedding is the ratio of the number of cube nodes used for the embedding and the number of mesh nodes. For meshes that cannot be embedded with minimal expansion and dilation one, the best known lower bound for the dilation is two. The bound of dilation two is tight for two-dimensional meshes [4]. The best known upper bound for the dilation is 7 for three-dimensional meshes [6], and $4k + 1$ for k-dimensional meshes, $k > 3$ [5].

We provide some minimal-expansion two-dimensional embeddings with dilation two, and lower average dilation than the general technique in [4]. We specify all length-two paths, and give the congestion, active-degree, and node-congestion of the embeddings. We give two three-dimensional embeddings with dilation two, and one three-dimensional embedding with dilation three, about half of the upper bound. We show how graph decomposition can be used to provide effective embeddings for many meshes, and how properties such as expansion, dilation, congestion, active-degree and node-congestion are affected by graph decomposition. We also compare the embeddings obtained by graph decomposition to the embeddings obtained by the modified line compression method in [4].

Embedding of meshes by graph decomposition was used implicitly in [12] to achieve dilation-two minimal-expansion embeddings of 87% of all two-dimensional meshes. Gray code embedding of one mesh was combined with direct embedding of one out of three small meshes. Below we extend these results by specifying all length-two paths to yield embeddings with a congestion of two. Both the average dilation and average congestion are one asymptotically. The graph decomposition technique in combination with previously known results [2,4,7,12] and some new direct embeddings yields dilation-two minimum-expansion embeddings of 96% of all three-dimensional meshes $\ell_1 \times \ell_2 \times \ell_3$, such that $1 \leq \ell_1, \ell_2, \ell_3 \leq 512$. By using Gray code embedding, only 29% of the meshes achieve minimal expansion for the considered three-dimensional domain.

The outline of this article is as follows. We first show how the dilation, expansion, congestion, active-degree and node-congestion of a graph represented as a product graph is related to the same properties of the graphs forming the product graph. Dilation-two, congestion-two, minimal-expansion embeddings of some small two-dimensional meshes used to form product graphs are given, as well as dilation-two, minimal-expansion embeddings of two small three-dimensional meshes, and a dilation-three embedding of one small three dimensional mesh. The reshaping and direct embedding techniques used for the embedding of these small meshes are briefly reviewed. Section 5 presents results for embedding of meshes by graph decomposition in combination with the reshaping and direct embedding techniques. Section 6 extends the results to meshes with wrap-around.

2 Preliminaries

For a graph G let $\mathcal{V}_G$ be its set of nodes, and $\mathcal{E}_G$ its set of edges. Let $|\mathcal{S}|$ denote the cardinality of a set $\mathcal{S}$, and $\lceil x \rceil_2$ and $\lfloor x \rfloor_2$ denote $2^{\lceil \log_2 x \rceil}$ and $2^{\lfloor \log_2 x \rfloor}$, respectively. The *embedding function* φ maps each node in the *guest graph* G into a unique node in the *host graph* H. The *expansion* ε of the mapping is $|\mathcal{V}_H|/|\mathcal{V}_G|$. The *relative expansion* for embedding a graph G into a hypercube H is $|\mathcal{V}_H|/\lceil |\mathcal{V}_G| \rceil_2$. Under the mapping function $\varphi : G \rightarrow H$, node $i \in \mathcal{V}_G$ is mapped to node $\varphi(i) \in \mathcal{V}_H$, and edge $e = (i,j) \in \mathcal{E}_G$ is mapped to a path $\varphi(e)$ consisting of the set of edges $\mathcal{E}_{\varphi(e)} = \{(\varphi(i), v_1), (v_1, v_2), \cdots, (v_{p-1}, \varphi(j))\} \subseteq \mathcal{E}_H$. The path $\varphi(e)$ has the node set $\mathcal{V}_{\varphi(e)} = \{\varphi(i), v_1, v_2, \cdots, v_{p-1}, \varphi(j)\}$. Let $dist(i,j)$ be the shortest path between nodes i and j in the considered graph. The *dilation* of the mapping φ is $\max(dist(\varphi(i), \varphi(j))$, for all $(i,j) \in \mathcal{E}_G$. The *dilation of an edge* $(i,j) \in \mathcal{E}_G$ is $dist(\varphi(i), \varphi(j))$, and the *average dilation* of the mapping φ is

$$\frac{1}{|\mathcal{E}_G|} \sum_{(i,j) \in \mathcal{E}_G} \{dist(\varphi(i), \varphi(j))\}.$$

The *congestion of an edge* $e' \in \mathcal{E}_H$ is $\sum_{e \in \mathcal{E}_G} |\{e'\} \cap \mathcal{E}_{\varphi(e)}|$, and the *congestion* of the embedding is

$$\max_{e' \in \mathcal{E}_H} \left\{ \sum_{e \in \mathcal{E}_G} \left| \{e'\} \cap \mathcal{E}_{\varphi(e)} \right| \right\}.$$

The *average congestion* of the embedding is similarly defined. The *node-congestion of a node* $v \in \mathcal{V}_H$ is $\sum_{e \in \mathcal{E}_G} |\{v\} \cap \mathcal{V}_{\varphi(e)}|$, and the *node-congestion* of the embedding is

$$\max_{v \in \mathcal{V}_H} \left\{ \sum_{e \in \mathcal{E}_G} \left| \{v\} \cap \mathcal{V}_{\varphi(e)} \right| \right\}.$$

The *average node-congestion* is defined similarly. The *adjacency node set* of a node $v \in \mathcal{V}_H$ is the set of nodes $\mathcal{V}_v = \{v_j \mid (v, v_j) \in \mathcal{E}_H\}$, and the *edge set of a node* $v \in \mathcal{V}_H$ is $\mathcal{E}_v = \{(v, v_j) \in \mathcal{E}_H\}$. The *active-degree of a node* v is $|\mathcal{E}_v \cap \{\cup_{e \in \mathcal{E}_G} \mathcal{E}_{\varphi(e)}\}|$, and the *active-degree* of the embedding is

$$\max_{v \in \mathcal{V}_H} \left| \mathcal{E}_v \cap \{\cup_{e \in \mathcal{E}_G} \mathcal{E}_{\varphi(e)}\} \right|.$$

The *average active-degree* is defined similarly.

If each node of the guest graph is mapped to a distinct node of the host graph, then the expansion is a measure of processor utilization. The slow down due to nearest-neighbor communication in the original graph being extended to communication along paths is a function of the length of the path and the congestion of the edges on the path. With a limited communications bandwidth at the nodes, the time for nearest-neighbor communication in the guest graph may also be influenced by the node-congestion and the active-degree.

A Boolean cube is a graph B with node set $\mathcal{V}_B$ such that $|\mathcal{V}_B| = 2^n$ for some n and edge set $\mathcal{E}_B = \{(i_{n-1} i_{n-2} \cdots i_j \cdots i_0, i_{n-1} i_{n-2} \cdots \bar{i}_j \cdots i_0) \mid j = \{0, 1, \cdots, n-1\}, i_j = \{0,1\}\}$; $|\mathcal{E}_B| = n 2^{n-1}$. The distance between nodes $i = (i_{n-1} i_{n-2} \cdots i_0)$ and $j = (j_{n-1} j_{n-2} \cdots j_0)$ in an n-cube is $Hamming(i,j) = \sum_{m=0}^{n-1} (i_m \oplus j_m)$, where $\oplus$ is the exclusive-or function. In the following, subcube 0 denotes the subcube that consists of all the nodes with the most significant bit of its address being 0. Subcube 1 is defined accordingly.

2.1 Graph decomposition

In this section we state and prove a few properties of product graphs, and the embedding characteristics of the product graph as a function of the embedding characteristics of the graphs forming the product graph.

Definition 1 The (Cartesian) *product* graph $G_1 \times G_2$ of a graph G_1 and a graph G_2 is defined as

$$\begin{aligned} \mathcal{V}_{G_1 \times G_2} &= \{[v_i, v_j] \mid \forall v_i \in \mathcal{V}_{G_1}, v_j \in \mathcal{V}_{G_2}\}, \text{ and} \\ \mathcal{E}_{G_1 \times G_2} &= \{([v_i, v_j], [v_i, v_k]) \mid \forall v_i \in \mathcal{V}_{G_1}, (v_j, v_k) \in \mathcal{E}_{G_2}\} \\ &\quad \bigcup \{([v_j, v_i], [v_k, v_i]) \mid \forall v_i \in \mathcal{V}_{G_2}, (v_j, v_k) \in \mathcal{E}_{G_1}\}. \end{aligned}$$

$G_1 \times G_2$ can be derived by replacing each node of G_1 by G_2 and replacing each edge of G_1 by a set of edges connecting corresponding nodes of G_2. Note that $G_1 \times G_2 = G_2 \times G_1$, $|\mathcal{V}_{G_1 \times G_2}| = |\mathcal{V}_{G_1}| * |\mathcal{V}_{G_2}|$, and $|\mathcal{E}_{G_1 \times G_2}| = |\mathcal{V}_{G_1}| * |\mathcal{E}_{G_2}| + |\mathcal{V}_{G_2}| * |\mathcal{E}_{G_1}|$.

Theorem 1 *Let φ_i be an embedding function which maps a graph G_i into a graph H_i with expansion ε_i, dilation d_i, congestion c_i, active-degree a_i, and node-congestion c_i', for $i = \{1, 2\}$. Then, there exists an embedding function φ that maps the graph $G = G_1 \times G_2$ into the graph $H = H_1 \times H_2$ with expansion $\varepsilon = \varepsilon_1 \varepsilon_2$, dilation $d = \max(d_1, d_2)$, congestion $c = \max(c_1, c_2)$, node-congestion $c' \leq c_1' + c_2'$, and active-degree $a \leq a_1 + a_2$.*

Proof: We prove the theorem by constructing an embedding function φ. Let $\mathcal{S}_1^{v_i} = \{([u_j, v_i], [u_k, v_i]) | \forall (u_j, u_k) \in \mathcal{E}_{G_1}\}$ and $\mathcal{S}_2^{u_i} = \{([u_i, v_j], [u_i, v_k]) | \forall (v_j, v_k) \in \mathcal{E}_{G_2}\}$. Clearly,

$$\mathcal{E}_{G_1 \times G_2} = (\cup_{v_i \in \mathcal{V}_{G_2}} \mathcal{S}_1^{v_i}) \bigcup (\cup_{u_i \in \mathcal{V}_{G_1}} \mathcal{S}_2^{u_i}).$$

$\mathcal{S}_1^{v_i}$ is a copy of G_1 identified by node v_i in G_2. For the host graph H, we define $\mathcal{T}_1^{v_i}$ and $\mathcal{T}_2^{u_i}$ similarly. Hence,

$$\mathcal{E}_{H_1 \times H_2} = (\cup_{v_i \in \mathcal{V}_{H_2}} \mathcal{T}_1^{v_i}) \bigcup (\cup_{u_i \in \mathcal{V}_{H_1}} \mathcal{T}_2^{u_i}).$$

An embedding function φ is derived from φ_1 and φ_2 by letting any edge $([u_j, v_i], [u_k, v_i]) \in \mathcal{S}_1^{v_i}$ corresponding to the edge $(u_j, u_k) \in \mathcal{E}_{G_1}$ be mapped to the path

$$\begin{aligned} &\{([\varphi_1(u_j), \varphi_2(v_i)], [w_1, \varphi_2(v_i)]), ([w_1, \varphi_2(v_i)], [w_2, \varphi_2(v_i)]), \cdots, \\ &\quad ([w_{p-1}, \varphi_2(v_i)], [\varphi_1(u_k), \varphi_2(v_i)])\} \subseteq \mathcal{T}_1^{\varphi_2(v_i)} \end{aligned}$$

in H, where the edge $(u_j, u_k) \in \mathcal{E}_{G_1}$ is mapped to the path

$$\varphi_1((u_j, u_k)) = \{(\varphi_1(u_j), w_1), (w_1, w_2), \cdots, (w_{p-1}, \varphi_1(u_k))\}$$

in H_1. The mapping of edges in $S_2^{v_i}$ are defined analogously. The dilation of any edge in $S_1^{v_i}$ is the same as the dilation of the corresponding edge in $\mathcal{E}_{G_1}$, and the dilation of any edge in $S_2^{v_i}$ is the same as that of the corresponding edge in $\mathcal{E}_{G_2}$. From the definition of φ it follows that any edge $e \in \mathcal{S}_1^{v_i}$, $\varphi(e) \subseteq \mathcal{T}_1^{\varphi_2(v_i)}$. From the definition of a product graph it follows that copies of H_1 (H_2) identified by different nodes in H_2 (H_1) are disjoint. Therefore, the congestion of all edges in $H_1 \times H_2$ is preserved. It also follows that the the node-congestion

for a node under the embedding function φ is the sum of the node-congestion for the node under the two embedding functions φ_1 and φ_2. Similarly, the active-degree of a node in H is the sum of the active-degrees of the node due to the embedding functions φ_1 and φ_2. ∎

If the embedding function φ_i for $i = \{1, 2\}$ yields the average dilation $\bar{d}_i$, the average congestion $\bar{c}_i$, the average node-congestion $\bar{c}'_i$, and the average active-degree $\bar{a}_i$ and

$$\alpha = \frac{|\mathcal{V}_{G_1}| * |\mathcal{E}_{G_2}|}{|\mathcal{E}_{G_1 \times G_2}|} \text{ and } \beta = \frac{|\mathcal{V}_{H_1}| * |\mathcal{E}_{H_2}|}{|\mathcal{E}_{H_1 \times H_2}|},$$

then, the embedding function φ has the average dilation $\bar{d} = \alpha\bar{d}_2 + (1 - \alpha)\bar{d}_1$, the average congestion $\bar{c} = \beta\bar{c}_2 + (1 - \beta)\bar{c}_1$, the average node-congestion $\bar{c}' = \bar{c}'_1 + \bar{c}'_2$, and the average active-degree $\bar{a} = \bar{a}_1 + \bar{a}_2$.

Corollary 1 *Let φ_i, $1 \leq i \leq r$, be embedding functions that maps graphs G_i into n_i-cubes with expansion ε_i, dilation d_i, congestion c_i, node-congestion c'_i, and active-degree a_i. Then, there exists an embedding function φ which maps a graph $G_1 \times G_2 \times \cdots \times G_r$ into a $\sum_{i=1}^{r} n_i$-cube with expansion $\varepsilon = \prod_{i=1}^{r} \varepsilon_i$, dilation $d = \max_i d_i$, congestion $c = \max_i c_i$, node-congestion $c' \leq \sum_{i=1}^{r} c'_i$, and active-degree $a \leq \sum_{i=1}^{r} a_i$.*

The fact that the dilation for the embedding of a product graph is the maximum dilation for the embedding of any graph used for the composition was observed in [18,21,16] and [9]. The corollary is used implicitly in [13] for the embedding of meshes by binary-reflected Gray codes, and in [7] and [12] for the embedding of two-dimensional meshes by a combination of direct embedding and Gray code embedding.

Corollary 2 *Let φ_i be an embedding function which maps an $\ell_{i1} \times \ell_{i2} \times \cdots \times \ell_{ik}$ mesh M_i into an n_i-cube with expansion ε_i, dilation d_i, congestion c_i, node-congestion c'_i, and active-degree a_i for $1 \leq i \leq r$. Then, there exists an embedding function φ which maps an $\ell_1 \times \ell_2 \times \cdots \times \ell_k$ mesh M into a $(\sum_{i=1}^{r} n_i)$-cube with expansion $\varepsilon = \prod_{i=1}^{r} \varepsilon_i$, dilation $d = \max_i d_i$, congestion $c = \max_i c_i$, node-congestion $c' \leq \sum_{i=1}^{r} c'_i$, and active-degree $a \leq \sum_{i=1}^{r} a_i$. where $\ell_j = \prod_{i=1}^{r} \ell_{ij}$ for $1 \leq j \leq k$.*

Proof: It follows from Corollary 1 and the two facts below:

- The product graph of an $\ell_1 \times \ell_2 \times \cdots \times \ell_k$ mesh and an $\ell'_1 \times \ell'_2 \times \cdots \times \ell'_{k'}$ mesh is an $\ell_1 \times \ell_2 \times \cdots \times \ell_k \times \ell'_1 \times \ell'_2 \times \cdots \times \ell'_{k'}$ mesh.
- [19] An $\ell_1 \times \ell_2 \times \cdots \times \ell_k$ mesh is a subgraph of the mesh

$$(\ell_{11} \times \ell_{21} \times \cdots \times \ell_{r1}) \times (\ell_{12} \times \ell_{22} \times \cdots \times \ell_{r2}) \times \cdots \times (\ell_{1k} \times \ell_{2k} \times \cdots \times \ell_{rk}),$$

$$\text{if } \prod_{i=1}^{r} \ell_{ij} = \ell_j, \ \forall 1 \leq j \leq k. \quad \blacksquare$$

The embedding function φ for an $\ell_1 \times \ell_2 \times \cdots \times \ell_k$ mesh M being a subgraph of $M_1 \times M_2$, where M_1 is the mesh $\ell_{11} \times \ell_{12} \times \cdots \times \ell_{1k}$, M_2 is the mesh $\ell_{21} \times \ell_{22} \times \cdots \times \ell_{2k}$, and

$\ell_i = \ell_{1i} \times \ell_{2i}$, $1 \leq i \leq k$, is defined in terms of the embedding functions φ_1 for M_1 and φ_2 for M_2. Let $z = (z_1, z_2, \cdots, z_k), 0 \leq z_i < \ell_i$ be a node in M, $x = (x_1, x_2, \cdots, x_k), 0 \leq x_i < \ell_{1i}$ be a node in M_1, $y = (y_1, y_2, \cdots, y_k), 0 \leq y_i < \ell_{2i}$ be a node in M_2, and $z_i = y_i \ell_{1i} + x_i, 1 \leq i \leq k$. The embedding of axis i of M consists of the embedding of ℓ_{2i} instances of axis ℓ_{1i}. Define

$$\tilde{\varphi}_1(y_1, y_2, \cdots, y_k, x_1, x_2, \cdots, x_k) = \varphi_1((x'_1, x'_2, \cdots, x'_k)) \text{ where } x'_i = \begin{cases} x_i, & \text{if } y_i \text{ is even,} \\ \ell_{1i} - 1 - x_i, & \text{otherwise.} \end{cases}$$

The function $\tilde{\varphi}_1$ differs from the function φ_1 in that a reflection of the embedding of axis i of M_1 is performed for instances for which y_i is odd. The function φ is defined as follows:

$$\varphi((z_1, z_2, \cdots, z_k)) = \varphi_2((y_1, y_2, \cdots, y_k)) || \tilde{\varphi}_1(y_1, y_2, \cdots, y_k, x_1, x_2, \cdots, x_k),$$

where "||" is the concatenation operator. If $\ell_{1i} = 2^{n_i}$, then a binary-reflected Gray code G is used for each axis of M_1 and $\varphi_1((x_1, x_2, \cdots, x_k)) = G(x_1)||G(x_2)|| \cdots ||G(x_k)$. The embedding function φ takes the form:

$$\begin{aligned} \varphi((z_1, z_2, \cdots, z_k)) &= \varphi_2((y_1, y_2, \cdots, y_k)) || \tilde{G}(y_1, x_1) || \tilde{G}(y_2, x_2) || \cdots || \tilde{G}(y_k, x_k), \\ \text{where } \tilde{G}(y_i, x_i) &= \begin{cases} G(x_i), & \text{if } y_i \text{ is even,} \\ G(2^{n_i} - 1 - x_i), & \text{otherwise.} \end{cases} \end{aligned} \quad (1)$$

An instance of axis i of mesh M_1 is traversed for every node along axis i of M_2. All edges along axis i of M_1 have dilation one for every i. With a dilation d embedding of mesh M_2 there exists at least one edge for some i that has dilation d for mesh M_2. By performing the embedding of axis i of the mesh M by traversing all edges along axis i of mesh M_1 for every edge of axis i of mesh M_2 the average dilation is minimized. Let $\bar{d}_2(i)$ be the average dilation of the edges of axis i in the mesh M_2, then the average dilation of the embedding of the mesh M is

$$1 + \sum_{i=1}^{k} \left\{ (\bar{d}_2(i) - 1) 2^{(\sum_{j=1}^{k} n_j) - n_i} (\ell_{2i} - 1) (\prod_{j=1}^{k} \ell_{2j}) / \ell_{2i} \right\} \Big/ \sum_{i=1}^{k} \left\{ (\ell_{2i} 2^{n_i} - 1) (\prod_{j=1}^{k} \ell_{2j} 2^{n_j}) / (\ell_{2i} 2^{n_i}) \right\}$$

$$\approx 1 + \sum_{i=1}^{k} \frac{\bar{d}_2(i) - 1}{k 2^{n_i}}.$$

The approximated term shows that the average dilation decreases as the length of axis i of mesh M_1 increases.

2.2 Dilation one embeddings

The following theorem due to Havel and Móravek [11] shows that for certain meshes, embedding with minimal expansion and dilation one is impossible.

Theorem 2 [11] *If an $\ell_1 \times \ell_2 \times \cdots \times \ell_k$ mesh is embedded in an n-cube with dilation one, then $n \geq \sum_{i=1}^{k} \lceil \log_2 \ell_i \rceil$.*

Theorem 2 was independently rediscovered in [3,8,12] and [10]. From the theorem follows that the expansion is in the range of 1 to 2^k. The percentage of meshes for which Gray code embedding [3,13,14,20] yields minimal-expansion embeddings decreases with the number

of axes of the mesh. Determining the asymptotic expansion for Gray code embedding is transformed to the following probability problem. Let a_i, $i \geq 1$, be a variable uniformly distributed over an interval $(\frac{1}{2}, 1]$, and a_i and a_j be independent variables for all $i \neq j$. Then, the probability that $\prod_{i=1}^{k} a_i \in (1/2^{\beta+1}, 1/2^{\beta}]$ is the asymptotic fraction of embedding k-dimensional meshes using Gray code embedding with an expansion 2^{β}. For minimal expansion $\beta = 0$.

Let $\alpha \in (\frac{1}{2}, 1]$ and $f_k(\alpha)$ be the probability that $\alpha \leq \prod_{i=1}^{k} a_i \leq 1$. Then,

Lemma 1 *$f_n(\alpha) = 2^n(1 - \alpha \sum_{i=0}^{n-1} \frac{(-1)^i \ln^i \alpha}{i!})$ for $\frac{1}{2} \leq \alpha \leq 1$.*

Proof: By induction on n. $f_1(\alpha) = 2(1 - \alpha)$, $\frac{1}{2} \leq \alpha \leq 1$.

$$
\begin{aligned}
f_{n+1}(\alpha) &= 2\int_{\alpha}^{1} f_n\left(\frac{\alpha}{x}\right) dx \\
&= 2\int_{\alpha}^{1} \left(2^n - 2^n \frac{\alpha}{x} \sum_{i=0}^{n-1} \frac{(-1)^i \ln^i \frac{\alpha}{x}}{i!}\right) dx \qquad (2) \\
&= 2^{n+1}\int_{\alpha}^{1} dx - 2^{n+1}\alpha \sum_{i=0}^{n-1} \int_{\ln \alpha}^{0} \frac{(-1)^i u^i}{i!} du \qquad (3) \\
&= 2^{n+1} - 2^{n+1}\alpha - 2^{n+1}\alpha \sum_{i=1}^{n} \frac{(-1)^i \ln^i \alpha}{i!} \\
&= 2^{n+1} - 2^{n+1}\alpha \sum_{i=0}^{n} \frac{(-1)^i \ln^i \alpha}{i!}.
\end{aligned}
$$

From Equation 2 to 3, we let $u = \ln \frac{\alpha}{x}$. Hence, $du = -\frac{dx}{x}$. ∎

Theorem 3 *The fraction of all k-dimensional meshes for which a binary-reflected Gray code embedding yields minimum expansion is $f_k(\frac{1}{2}) = 2^k(1 - \frac{1}{2}\sum_{i=0}^{k-1} \frac{\ln^i 2}{i!})$, asymptotically.*

Proof: By Lemma 1. ∎

Figure 1 shows $f_k(\frac{1}{2})$ as a function of the number of dimensions, k. $f_2(\frac{1}{2}) = 2(1 - \ln 2) \approx 0.61$ and $f_3(\frac{1}{2}) = 4(1 - \ln 2 - \frac{\ln^2 2}{2}) \approx 0.27$.

3 Reshaping techniques

Reshaping an $\ell_1 \times \ell_2 \times \cdots \times \ell_k$ mesh is the embedding of the mesh in an $\ell'_1 \times \ell'_2 \times \cdots \times \ell'_k$ mesh. The number of axes is preserved, but the length of the different axes are changed. We only consider reshaping an $\ell_1 \times \ell_2$ mesh into an $N_1 \times N_2$ mesh, where $N_1 = 2^{n_1}$ and $N_2 = 2^{n_2}$, such that $N_1 N_2 = \lceil \ell_1 \ell_2 \rceil_2$, and $\ell_1 \leq \ell_2$. The embedding can be represented by joining corresponding nodes on ℓ_1 lines of length $\ell_2 - 1$. Step embedding [1] and a modified step embedding yield dilation three. Folding [17], line compression [1], and modified line compression [4] yield dilation two. Embeddings of a multidimensional mesh into another multidimensional mesh of different shape and cardinality are studied in [15] and [19]. By making the reshaped mesh having axes with lengths being powers of two, a Gray code embedding can be applied to the reshaped mesh [13].

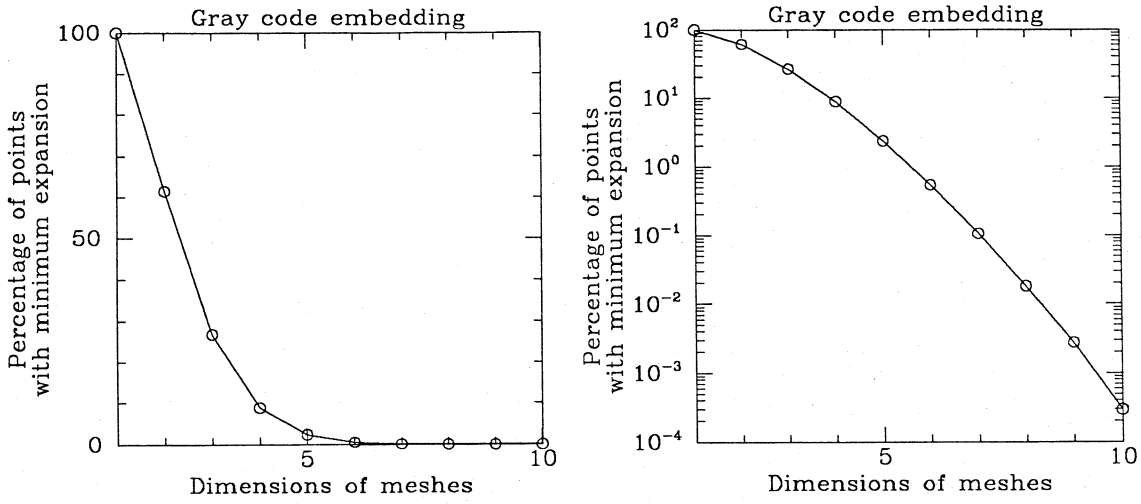

Figure 1: The asymptotic fraction of the domain $(\lceil \ell_i \rceil_2/2) < \ell_i \leq \lceil \ell_i \rceil_2$ for which minimum expansion is attained by Gray code embedding. The right plot has a logarithmic scale for the y-axis.

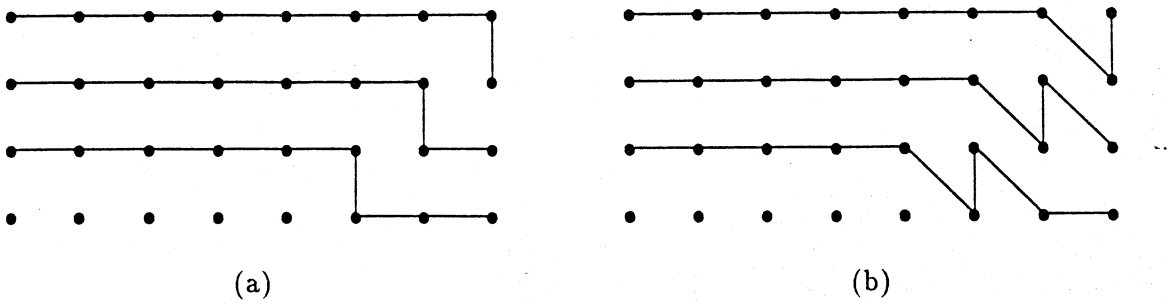

Figure 2: Embedding of a 3×9 mesh into a 4×8 mesh by step embedding with, (a) dilation 3, (b) dilation 2.

3.1 Step embedding

Let $N_1 = \lceil \ell_1 \rceil_2$ and $N_2 = \lfloor \ell_2 \rfloor_2$. Each row of the guest mesh will "turn" at some point and make a vertical traversal [1]. Figure 2-(a) shows the embedding of a 3×9 mesh into a 4×8 mesh. Different rows traverse different columns. It follows that $N_2 \geq \ell_1$. Row i of the guest mesh occupies a part of rows i and $i + \ell_2 - N_2$ of the host mesh, and $N_1 \geq \ell_2 - N_2 + \ell_1$. The dilation is three. The number of edges with dilation 3 is $(\ell_2 - N_2)(\ell_1 - 1)$. The average dilation is $1 + \frac{2(\ell_2 - N_2)(\ell_1 - 1)}{|E_G|} \approx 1 + \frac{\ell_2 - N_2}{\ell_2}$, which is in the range of 1 to 1.5. For certain meshes, for instance if $\ell_2 = N_2 + 1$, the dilation can be reduced to 2 as shown in 2-(b). Figure 15-(b) shows the pairs (ℓ_1, ℓ_2) for which the step embedding method attains minimal expansion, while Gray code embedding cannot. The ratio of the number of these pairs to the total number of pairs is $\approx \frac{1}{8}$.

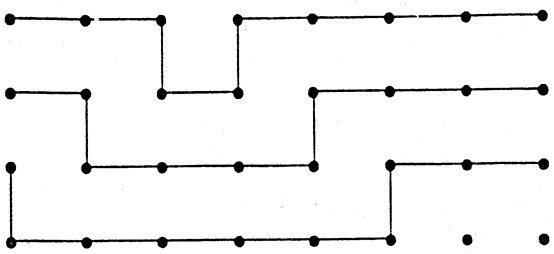

Figure 3: Embedding of a 3×10 mesh into a 4×8 mesh by modified step embedding.

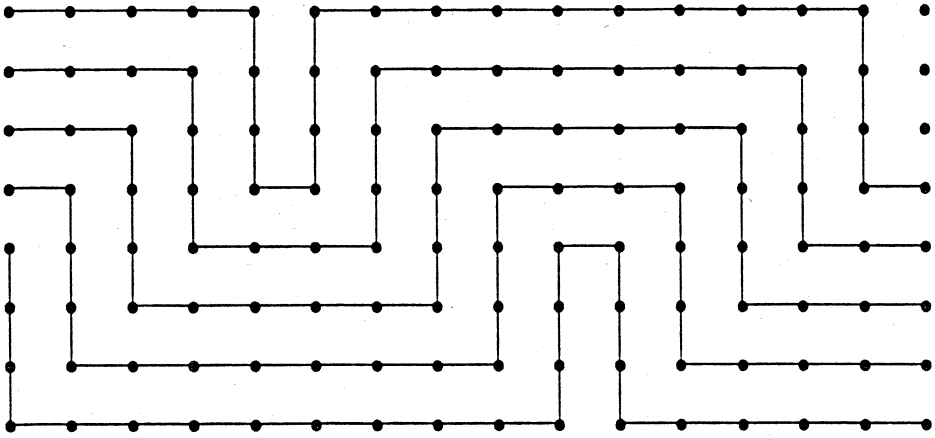

Figure 4: Embedding of a 5×25 mesh into a 8×16 mesh by modified step embedding.

3.2 Modified step embeddings

In step embedding, a row of the guest mesh only makes one vertical traversal. In modified step embedding, several vertical traversals are allowed, Figures 3 and 4. Each vertical traversal involves ℓ_1 distinct columns, one for each row, and the maximum number of vertical traversals by all rows is $\alpha = \lfloor \frac{N_2}{\ell_1} \rfloor$. Since each vertical traversal can save $N_1 - \ell_1$ nodes from the second axis, the condition $N_1 \geq \lceil \frac{\ell_2 - N_2}{\alpha} \rceil + \ell_1$ must hold. Note that the step embedding technique cannot be applied if $\alpha = 0$, i.e., $N_2 < \ell_1$. For $\alpha = 1$ the modified step embedding technique degenerates to the step embedding technique.

The modified step embedding allows minimal expansion for more pairs (ℓ_1, ℓ_2) than step embedding, Figure 15-(c). The additional pairs all satisfy the condition $\lceil \ell_2 \rceil_2 / \lceil \ell_1 \rceil_2 \geq 4$ (assuming $\ell_1 \leq \ell_2$). For example, a 3×10 mesh is mapped to a 5×8 mesh by step embedding, but to a 4×8 mesh by modified step embedding, Figure 3. A 5×25 mesh is mapped to a 14×16 mesh by step embedding, but a 8×16 mesh by modified embedding, Figure 4. The average dilation is the same as in step embedding, i.e., 1 to 1.5. If the number of vertical traversals k satisfies the condition $\lceil \frac{\ell_2 - N_2}{2} \rceil \leq k \leq \ell_2 - N_2$ then the dilation is 2. However, the average dilation will increase.

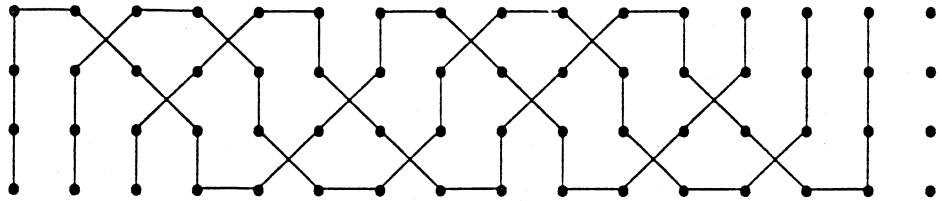

Figure 5: Embedding of a 3×20 mesh into a 4×16 mesh by folding.

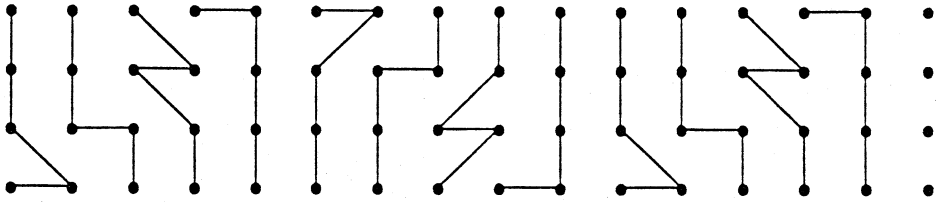

Figure 6: Embedding of a 5×12 mesh into a 4×16 mesh by the line compression method.

3.3 Folding

In [1] the break-and-fold technique [17] was used to square-up an $\ell_1 \times \ell_2$ mesh with $\ell_1 \ll \ell_2$. If there exists an n_1-cube and an n_2-cube such that $N_1 N_2 = \lceil \ell_1 \ell_2 \rceil_2$, $N_1 > \ell_1$ and $\lfloor \frac{N_2}{\ell_1} \rfloor \geq \lceil \frac{\ell_2}{N_1} \rceil$, then the break-and-fold technique will yield a minimal expansion embedding. Figure 5 shows the embedding of a 3×20 mesh into a 4×16 mesh. The dilation of the embedding is two. Figure 15-(d) shows the pairs (ℓ_1, ℓ_2) for which the folding technique yields minimal expansion, but the Gray code embedding does not. The set of these pairs is mostly disjoint from the set of pairs for which step embedding yields minimal expansion, but the Gray code does not. However, folding and the modified step embedding largely covers the same pairs as the folding technique. The average dilation is $\approx 1 + \frac{\ell_1}{N_2}$.

3.4 Line compression

Line compression is also adopted from [1] in which a basic "tile" of size $a \times b$ is compressed into a tile of size $b \times a$. Let $b = a + 1$, then $\lfloor \frac{N_2}{a} \rfloor \geq \ell_2 - N_2$ and $N_1 \geq \ell_1 + \lceil \frac{\ell_1}{a} \rceil$. In order to satisfy these two constraints, $a > 1$ and $\ell_2 \leq \frac{3}{2} N_2$ must be satisfied. One can easily show that any $(2^x - 1) \times (2^x + 1)$ mesh can be reshaped into a $2^x \times 2^x$ mesh by line compression (with $a = 2^x - 1$). The dilation is two and the average dilation is $\approx 1 + \frac{a+2b}{2ab} \approx 1 + \frac{3}{2a}$. Minimizing the average dilation is equivalent to maximizing a. Figure 6 shows the embedding of a 5×12 mesh into a 4×16 mesh by the line compression method. In this figure solid lines represent columns of the guest mesh. Figure 15-(e) shows the pairs (ℓ_1, ℓ_2) for which the line compression method yields minimal expansion, but the Gray code does not. The set of these pairs include mostly the set of pairs for which (a) step embedding, (b) modified step embedding, and (c) folding yields minimal expansion, but Gray code does not.

3.5 Modified line compression

A dilation-two embedding for all two-dimensional meshes is given by Chan [4]. The technique is based on a modification of the line compression technique. An intermediate mesh of the form $\lfloor \ell_1 \rfloor_2 \times \lceil \ell_2 \rceil_2$ is mapped to the guest mesh $\ell_1 \times \ell_2$ to cover all the nodes of the guest mesh. The intermediate mesh can be embedded in the Boolean cube by a binary-reflected Gray code. Each row of the intermediate mesh forms a chain of length up to $\lceil \ell_2 \rceil_2$ and all the $\lfloor \ell_1 \rfloor_2$ chains together cover all the nodes of the guest mesh. Any two adjacent nodes in the guest mesh are either covered by the same chain or two successive chains. If they are covered by the same chain, then the distance along the chain is at most two (which implies dilation two); otherwise, they are within distance three. With a binary-reflected Gray code encoding of each chain in the Boolean cube, dilation three is achieved. To reduce the dilation to two, each chain is embedded into two symmetrical subcubes. Every two successive nodes in a chain are assigned to corresponding positions of the two symmetrical subcubes. The order in which successive nodes are assigned to these two subcubes is based on a coloring technique (on a derived bipartite graph) such that the distance between any two corresponding nodes of adjacent nodes in the guest mesh is at most two. Though both the dilation and expansion are minimal, the technique does not necessarily guarantee minimal congestion, node-congestion, or average dilation.

4 Direct cube embeddings

In this section we first give three dilation-two, minimal-expansion embeddings of two-dimensional meshes in Boolean cubes [12], then two dilation-two and one dilation-three, minimal-expansion embeddings of three-dimensional meshes. The meshes are of shapes 3×5, 7×9, 11×11, $3 \times 3 \times 3$, $3 \times 3 \times 7$ and $5 \times 5 \times 5$. These two-dimensional meshes allows for minimal expansion and dilation embeddings for all two-dimensional meshes in five-dimensional Boolean cubes, and six-dimensional cubes with the exception of the embedding of the mesh 3×21. A comparison of the characteristics of the embedding with those of the other embedding techniques is made.

4.1 Two-dimensional direct embeddings

All three two-dimensional embeddings have the property that the dilation for any edge of the upper-left $\lfloor \ell_1 \rfloor_2 \times \lfloor \ell_2 \rfloor_2$ submesh of the $\ell_1 \times \ell_2$ mesh, is one.

Embedding a 3×5 mesh into a 4-cube. To embed a 3×5 mesh into a 4-cube, we use the mapping represented by Figure 7, in which the numbers represent the addresses of the cube nodes to which the mesh nodes are mapped. For ease of determining the dilation of edges, we use $\overline{x}$ to represent the node in subcube one that corresponds to node x in subcube zero, i.e., $\overline{x}$ is derived from x by complementing the most significant bit. The '•' sign on the dashed line means that the Hamming distance between the two adjacent mesh nodes is two when embedded in the cube. From Figure 7 it is apparent that the dilation is two.

To determine the congestion of the embedding, we specify all length-two paths as follows, where the '•' sign above a doubled arrow denotes a cube edge, which is also used as a

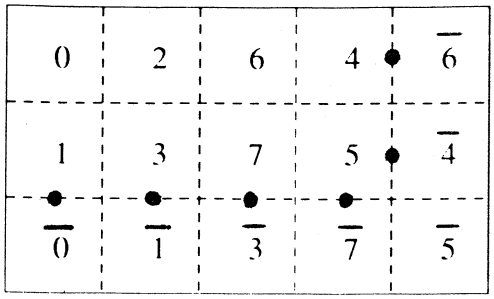

Figure 7: Embedding of a 3×5 mesh in a 4-cube.

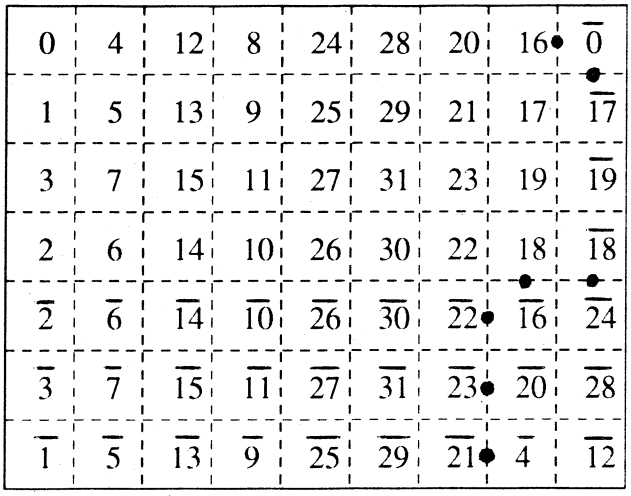

Figure 8: Embedding of a 7×9 mesh in a 6-cube.

dilation-one edge.

$\overline{0} \leftrightarrow 0 \overset{\bullet}{\leftrightarrow} 1$, $\overline{1} \leftrightarrow 1 \overset{\bullet}{\leftrightarrow} 3$, $\overline{3} \leftrightarrow 3 \overset{\bullet}{\leftrightarrow} 7$,
$\overline{7} \leftrightarrow 7 \overset{\bullet}{\leftrightarrow} 5$, $\overline{4} \leftrightarrow 4 \overset{\bullet}{\leftrightarrow} 5$, $\overline{6} \leftrightarrow 6 \overset{\bullet}{\leftrightarrow} 4$.

By inspection, one can easily show that the congestion is two; the number of cube edges with congestion two is 6; the active-degree is 4; and the node-congestion is 6. The embedding of a $3 \cdot 2^{n_1} \times 5 \cdot 2^{n_2}$ mesh was also independently found in [7]. The 5×12 mesh embedded by line compression, Figure 6, contains the embedding of 3×5 meshes.

Embedding of a 7×9 mesh into a 6-cube. Figure 8 shows the embedding of a 7×9 mesh in a 6-cube. The length-two paths in the cube are specified as follows:

$\overline{4} \leftrightarrow \overline{5} \leftrightarrow \overline{21}$. $\overline{20} \leftrightarrow \overline{21} \overset{\bullet}{\leftrightarrow} \overline{23}$. $\overline{16} \leftrightarrow \overline{18} \leftrightarrow \overline{22}$.
$\overline{16} \leftrightarrow 16 \leftrightarrow 18$. $\overline{24} \leftrightarrow \overline{26} \leftrightarrow \overline{18}$. $\overline{0} \leftrightarrow \overline{16} \leftrightarrow \overline{17}$.
$\overline{0} \leftrightarrow 0 \leftrightarrow 16$.

By inspection, the dilation is two; the number of edges with dilation two is 7; the congestion is two; the number of edges with congestion two is one; the active-degree is 6

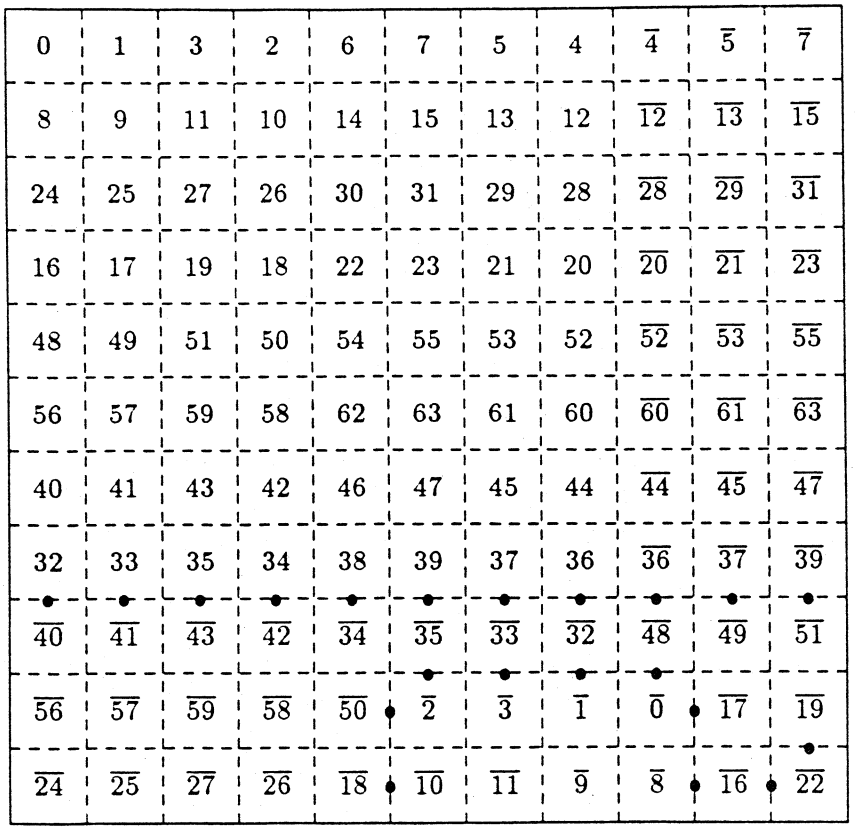

Figure 9: Embedding of an 11 × 11 mesh in a 7-cube.

(for node $\overline{16}$); and the node-congestion is 6.

Embedding of an 11 × 11 mesh into a 7-cube. Figure 9 shows the embedding of an 11 × 11 mesh in a 7-cube. The length-two paths are specified as follows:

$\overline{51} \leftrightarrow \overline{55} \leftrightarrow \overline{39}$,
$\overline{48} \leftrightarrow \overline{16} \leftrightarrow \overline{0}$,
$\overline{16} \leftrightarrow \overline{20} \leftrightarrow \overline{22}$,
$\overline{32} \overset{\bullet}{\leftrightarrow} \overline{33} \leftrightarrow \overline{1}$,
$\overline{35} \leftrightarrow \overline{39} \leftrightarrow 39$,
$\overline{18} \overset{\bullet}{\leftrightarrow} \overline{26} \leftrightarrow \overline{10}$,
$\overline{43} \leftrightarrow \overline{35} \leftrightarrow 35$,

$\overline{49} \leftrightarrow \overline{53} \leftrightarrow \overline{37}$,
$\overline{0} \overset{\bullet}{\leftrightarrow} \overline{1} \leftrightarrow \overline{17}$,
$\overline{22} \leftrightarrow \overline{23} \leftrightarrow \overline{19}$,
$\overline{33} \leftrightarrow \overline{37} \leftrightarrow 37$,
$\overline{35} \overset{\bullet}{\leftrightarrow} \overline{34} \leftrightarrow \overline{2}$,
$\overline{34} \leftrightarrow \overline{38} \leftrightarrow 38$,
$\overline{41} \leftrightarrow \overline{33} \leftrightarrow 33$,

$\overline{48} \leftrightarrow \overline{52} \leftrightarrow \overline{36}$
$\overline{8} \leftrightarrow \overline{24} \leftrightarrow \overline{16}$
$\overline{32} \leftrightarrow 32 \leftrightarrow 36$
$\overline{33} \overset{\bullet}{\leftrightarrow} \overline{35} \leftrightarrow \overline{3}$
$\overline{50} \overset{\bullet}{\leftrightarrow} \overline{18} \leftrightarrow \overline{2}$
$\overline{42} \leftrightarrow 42 \overset{\bullet}{\leftrightarrow} 34$
$\overline{40} \leftrightarrow 40 \overset{\bullet}{\leftrightarrow} 32$

The length-two paths are all edge-disjoint with respect to each other. Hence, the congestion is at most two. By inspection, the dilation is two; the number of edges with dilation two is 21; the congestion is two; the number of edges with congestion two is 8 (marked by '•'); the active-degree is 6 (for instance, nodes $\overline{33}$ and $\overline{35}$); and the node-congestion is 8 (for instance, nodes $\overline{33}$ and $\overline{35}$).

Mesh	Technique	number of edges with			
		dil. 2	dil. 3	cong. 2	cong. 3
3×5	Step Embedding	0	2	6	0
	Folding	5	0	7	1
	Line Compression	6	0	6	1
	Modified Line Comp.	6	0	-	-
	Direct	6	0	6	0
7×9	Step Embedding	0	6	18	0
	Folding	ϕ	ϕ	ϕ	ϕ
	Line Compression	18	0	-	-
	Modified Line Comp.	21	0	-	-
	Direct	7	0	1	0
11×11	Step Embedding	ϕ	ϕ	ϕ	ϕ
	Folding	ϕ	ϕ	ϕ	ϕ
	Line Compression	81	0	-	-
	Modified Line Comp.	92	0	-	-
	Direct	21	0	8	0

Table 1: Comparison of some embedding characteristics for small meshes. "ϕ" means the embedding does not cover the considered mesh, and "-" denotes the omitted entries.

4.2 Comparison of embedding techniques for the 3×5, 7×9, and 11×11 meshes

All techniques yield dilation two, the minimal. However, the number of edges with dilation two and congestion two differs, and so does the active-degree and node-congestion. Not all techniques can be used for each mesh. Moreover, line compression can be performed in several ways. Likewise, there exist several ways in which the length-two paths can be specified. The number of edges with dilation two, or three, and congestion two, or three, in Table 1 is not necessarily minimal, but the best we know. In section 5 we will show how these characteristics are affected under decomposition, and the relevance of the model meshes for the embedding of two-dimensional meshes in small Boolean cubes.

4.3 Three-dimensional direct embeddings

All three embeddings in this section have the property that the Gray code embedding will not yield minimal expansion. The direct embedding of the $3 \times 3 \times 3$ and $3 \times 3 \times 7$ meshes have a dilation of two, and the embedding of the $5 \times 5 \times 5$ mesh has a dilation of three. All three embeddings have minimal expansion. Applying the reshaping technique, the direct two-dimensional embedding to any pair of the three dimensions, or the decomposition technique does not result in dilation-two, minimal-expansion embeddings.

Embedding of a $3 \times 3 \times 3$ mesh in a 5-cube. Figure 10 shows the embedding of a $3 \times 3 \times 3$ mesh in a 5-cube with dilation two. The number in the figure is the cube address in

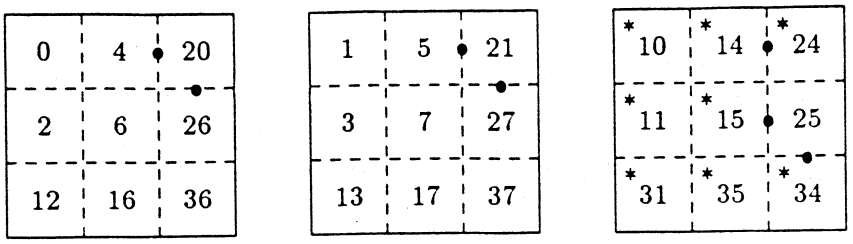

Figure 10: Embedding of a $3 \times 3 \times 3$ mesh in a 5-cube. The number is the cube address in octal representation to which the mesh node is mapped.

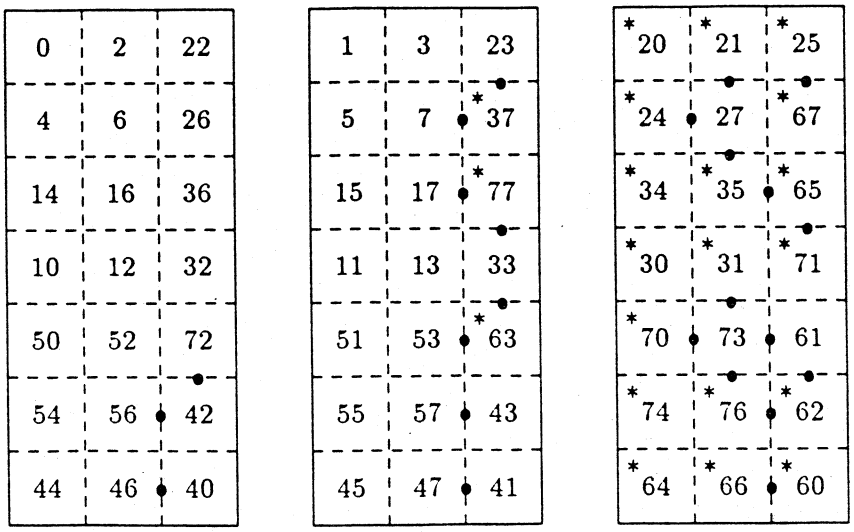

Figure 11: Embedding of a $3 \times 3 \times 7$ mesh in a 6-cube. The number is the cube address in octal representation to which the mesh node is mapped.

octal representation to which the mesh node is mapped. The sign "$*$" marks a dilation-two edge between the marked node and the corresponding node in the plane immediately to the left. The number of dilation-two edges is 15. The congestion is two; the number of edges with congestion two is 11; the active-degree is 6; and the node-congestion is 9.

Embedding of a $3 \times 3 \times 7$ mesh in a 6-cube. Figure 11 shows the embedding of a $3 \times 3 \times 7$ mesh in a 6-cube with dilation two. The number of dilation-two edges is 45.

Embedding of a $5 \times 5 \times 5$ mesh in a 7-cube. Figure 12 shows the embedding of a $5 \times 5 \times 5$ mesh in a 7-cube with dilation three. The numbers of dilation-two and dilation-three edges are 18 and 101, respectively.

4.4 Summary of direct embeddings

The characteristics of the direct embeddings are summarized in Table 2.

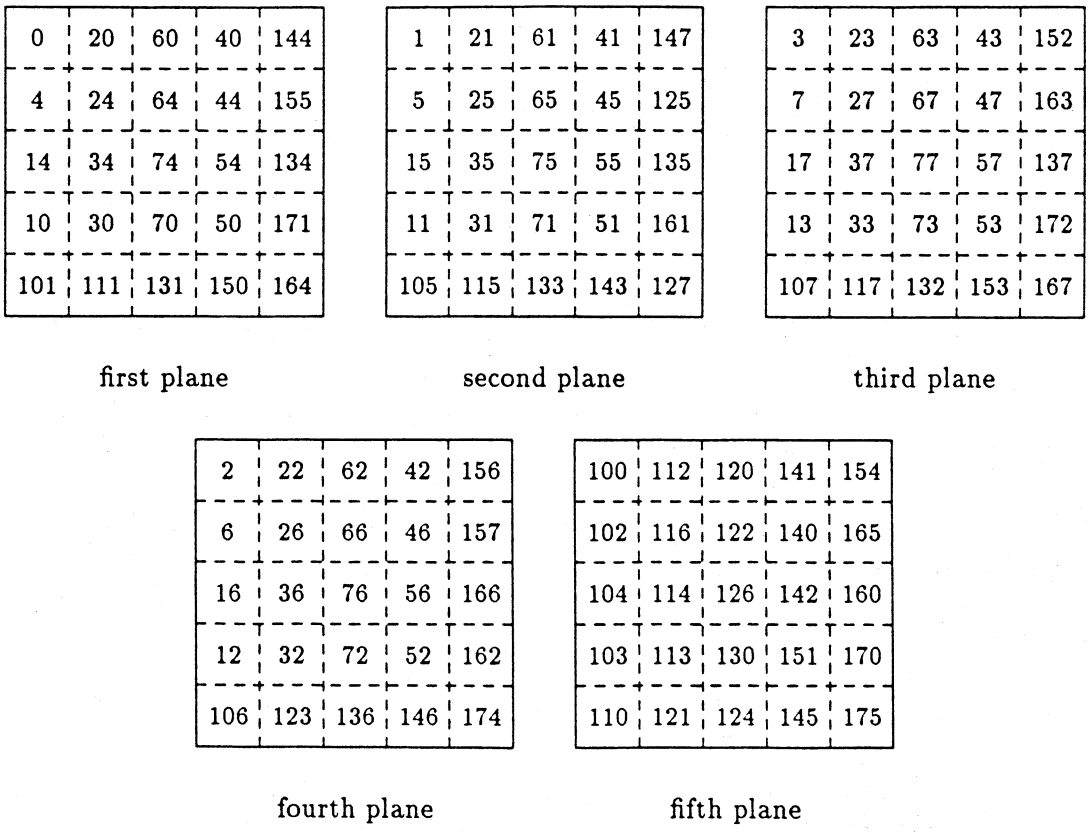

Figure 12: Embedding of a $5 \times 5 \times 5$ mesh in a 7-cube with dilation three. The number is the cube address in octal representation to which the mesh node is mapped.

Mesh	Dilation	Average dilation	Congestion	Average congestion	Active-degree	Node-congestion
3×5	2	1.27	2	1.27	4	6
7×9	2	1.06	2	1.01	6	6
11×11	2	1.10	2	1.04	6	8
$3 \times 3 \times 3$	2	1.28	2	1.20	6	9
$3 \times 3 \times 7$	2	1.33	-	-	-	-
$5 \times 5 \times 5$	3	1.73	-	-	-	-

Table 2: Summary of embedding characteristics for direct embeddings.

For the three-dimensional meshes of 128 nodes or less, the $5 \times 5 \times 5$ mesh is the only mesh for which we do not know of a minimal expansion dilation two embedding, if it exists. For three-dimensional meshes with up to 256 nodes, there are four additional meshes for which the same statement applies: $5 \times 7 \times 7$, $3 \times 9 \times 9$, $5 \times 5 \times 10$ and $3 \times 5 \times 17$.

5 Embedding by graph decomposition

The general strategy for mesh embedding by graph decomposition is the following:

1. If the number of nodes along any axis is a power of two then the embedding of all nodes along that axis is by a binary-reflected Gray code. For instance, the embedding of a $12 \times 16 \times 20 \times 32$ mesh is reduced to the problem of embedding a 12×20 and a 16×32 mesh.

2. For the axes with lengths not being powers of two, a decomposition is sought into meshes for which good embeddings are known, and the products of the expansions for the decomposed meshes is minimized. For instance, the embedding of a 12×20 mesh can be reduced to the embedding of a 3×5 and a 4×4 mesh. Embedding a $3 \times 25 \times 3$ mesh can be reduced to the embedding of two 3×5 meshes.

3. If the axes lengths are not powers of two, but can be increased slightly without increasing the size of the cube for a minimal expansion of the original mesh, then the mesh might be extended, and the procedure just mentioned applied to the extended mesh. For instance, a $3 \times 3 \times 23$ mesh can be extended to a $3 \times 3 \times 25$ mesh, which is treated with the scheme above.

Using the direct embeddings together with graph decomposition allows for minimal-expansion, dilation-two embedding of 70% of all two-dimensional meshes for which Gray code does not yield minimal expansion. For three-dimensional meshes, we use these direct embeddings extended with the two-dimensional result in [4], and the graph decomposition technique. We achieve dilation-two minimal-expansion embeddings for 96% of the three-dimensional meshes contained within, or equal to, a $512 \times 512 \times 512$ mesh.

5.1 Two-dimensional Meshes

Any technique, such as reshaping [13], direct embedding [12], or other technique [2,4,7,10] can be used in combination with the decomposition technique to reduce the average dilation and average congestion. The number of edges with dilation two for any of the reshaping techniques are approximately proportional to the size of the mesh for most known embeddings. For an $\ell_1 \times \ell_2$ mesh, the maximum of $n_1 + n_2$ is determined such that $\ell_i \leq \ell_i' 2^{n_i}$ and $\lceil \ell_1 \ell_2 \rceil_2 = \lceil \ell_1' \ell_2' 2^{n_1+n_2} \rceil_2$. Then, the problem is reduced to embedding an $\ell_1' \times \ell_2'$ mesh, which can always be done with minimal expansion and dilation two by the method in [4]. For instance, a 17×17 mesh can be extended to 24×20 mesh and then decomposed into a 3×5 mesh and a $2^3 \times 2^2$ mesh. Table 3 gives some examples of minimal-expansion dilation-two embeddings for cubes of up to six dimensions. Direct embeddings are required for meshes such that: both ℓ_1 and ℓ_2 are odd numbers, $\lceil \ell_1 \ell_2 \rceil_2 = 2^n$, and $\lceil \ell_1 \rceil_2 \lceil \ell_2 \rceil_2 = \lceil \ell_1 (\ell_2 + 1) \rceil_2 = \lceil (\ell_1 + 1) \ell_2 \rceil_2 = 2^{n+1}$.

4-cube		6-cube	
Mesh	Technique	Mesh	Technique
$1 \times \{16, 15, \cdots, 9\}$	Gray code	$1 \times \{64, 63, \cdots, 33\}$	Gray code
$2 \times \{8, 7, \cdots, 5\}$	Gray code	$2 \times \{32, 31, \cdots, 17\}$	Gray code
3×5	Direct	3×21	Direct
$3 \times \{4, 3\}$	Gray code	$3 \times 20 = (3 \times 5) \times (1 \times 4)$	Decomp.
4×4	Gray code	$3 \times \{19, 18, 17\} \rightarrow 3 \times 20$	Extension
		$3 \times \{16, 15, \cdots, 11\}$	Gray code
5-cube		$4 \times \{16, 15, \cdots, 9\}$	Gray code
Mesh	Technique	$5 \times 12 = (5 \times 3) \times (1 \times 4)$	Decomp.
$1 \times \{32, 31, \cdots, 17\}$	Gray code	$5 \times \{11, 10, 9\} \rightarrow 5 \times 12$	Extension
$2 \times \{16, 15, \cdots, 9\}$	Gray code	$5 \times \{8, 7\}$	Gray code
$3 \times 10 = (3 \times 5) \times (1 \times 2)$	Decomp.	$6 \times 10 = (3 \times 5) \times (2 \times 2)$	Decomp.
$3 \times 9 \rightarrow 3 \times 10$	Extension	$6 \times 9 \rightarrow 6 \times 10$	Extension
$3 \times \{8, 7, 6\}$	Gray code	$6 \times \{8, 7, 6\}$	Gray code
$4 \times \{8, 7, \cdots, 5\}$	Gray code	7×9	Direct
$5 \times 6 = (5 \times 3) \times (1 \times 2)$	Decomp.	$7 \times \{8, 7\}$	Gray code
$5 \times 5 \rightarrow 5 \times 6$	Extension	8×8	Gray code

Table 3: Embedding strategies for some two-dimensional meshes, $\ell_1 \leq \ell_2$.

Method	number of edges with	
	dil. 2	dil. 3
Step Embedding	0	10
Folding	ϕ	ϕ
Line Compression	20	0
Modified Line Compression	36	0
Decomposition	12	0

Table 4: Dilation of edges for the 6×10 mesh.

Figure 13 shows the embedding of meshes of the form $3 \cdot 2^{n_1} \times 5 \cdot 2^{n_2}$. In the figure, 'r' and 'c' denote the local addresses within a block (subcube). The local addresses are determined by a binary-reflected Gray code $\tilde{G}(x_i, y_i)$ as defined in Equation (1). Figure 14 shows a specific case: the embedding of a 6×10 mesh into a 6-cube. Table 4 shows how the different embedding methods compare for this particular mesh.

Figure 15-(f) shows the set of pairs (ℓ_1, ℓ_2) for which the decomposition of a mesh into a Boolean cube graph and a mesh with direct embedding given above yields lower expansion than a Gray code embedding. The ratio of the number of these pairs to the total number of pairs is $\approx \frac{1}{4}$, independent of the range of $2^n \times 2^n$. The average dilation is one, asymptotically. Table 5 gives the average dilation for meshes decomposed into a Boolean cube graph and a mesh for which a direct embedding is given above. The expansion is at most ≈ 2.4

0000rc	0010rc	0110rc	0100rc	1110rc
0001rc	0011rc	0111rc	0101rc	1100rc
1000rc	1001rc	1011rc	1111rc	1101rc

Figure 13: Block addresses of embedding a $3 \cdot 2^{n_1} \times 5 \cdot 2^{n_2}$ mesh into a $(4 + n_1 + n_2)$-cube.

000000	001010	001010	001000	011000	011010	010010	010000	111000	111010
000001	000011	001011	001001	011001	011011	010011	010001	111001	111011
000101	000111	001111	001101	011101	011111	010111	010101	110001	110011
000100	000110	001110	001100	011100	011110	010110	010100	110000	110010
100000	100010	100110	100100	101100	101110	111110	111100	110100	110110
100001	100011	100111	100101	101101	101111	111111	111101	110101	110111

Figure 14: Embedding of a 6×10 mesh into a 6-cube.

$\ell_1 \times \ell_2$ embedding	# of edges w. dil. 2	Average dilation	$\lfloor \ell_i \rfloor_2 = 16$	$\lfloor \ell_i \rfloor_2 = 128$	$\lfloor \ell_i \rfloor_2 = 1024$
$5 \cdot 2^{n_1} \times 3 \cdot 2^{n_2}$	$\frac{4}{5}\ell_1 + \frac{2}{3}\ell_2$	$1 + \frac{12\ell_1+10\ell_2}{15(2\ell_1\ell_2-\ell_1-\ell_2)}$	1.03	1.004	1.0005
$9 \cdot 2^{n_1} \times 7 \cdot 2^{n_2}$	$\frac{1}{3}\ell_1 + \frac{4}{7}\ell_2$	$1 + \frac{7\ell_1+12\ell_2}{21(2\ell_1\ell_2-\ell_1-\ell_2)}$	1.02	1.003	1.0003
$11 \cdot 2^{n_1} \times 11 \cdot 2^{n_2}$	$\frac{5}{11}\ell_1 + \frac{16}{11}\ell_2$	$1 + \frac{55\ell_1+176\ell_2}{121(2\ell_1\ell_2-\ell_1-\ell_2)}$	1.04	1.005	1.0007

Table 5: The average dilation for meshes embedded by graph decomposition into a Boolean cube graph and a mesh embedded by direct mesh embedding.

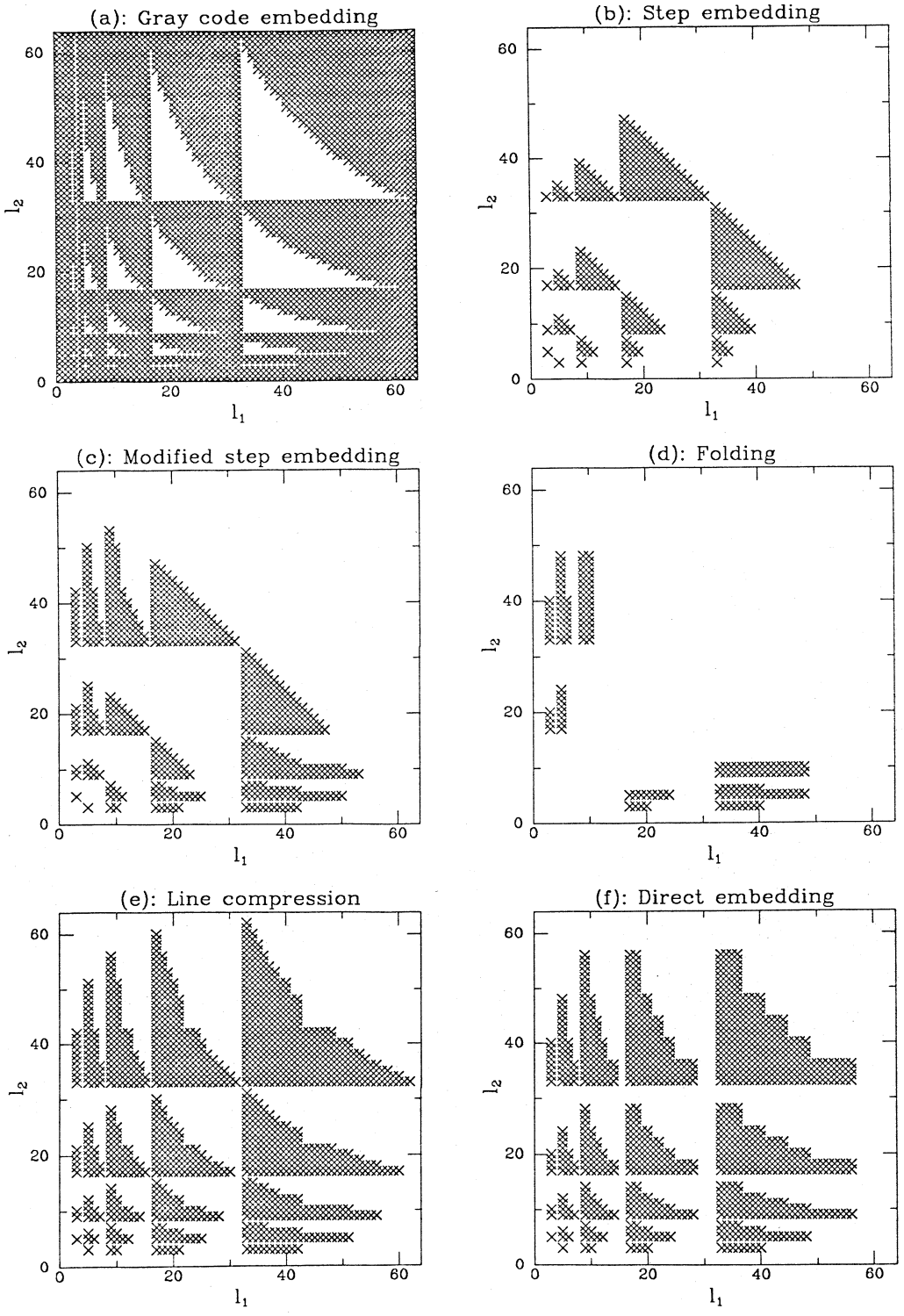

Figure 15: The pairs (ℓ_1, ℓ_2) for which minimal expansion is attained using (a) Gray code embedding, (b) step embedding, (c) modified step embedding, (d) folding, (e) line compression, and (f) direct embedding. For (b) to (f), only the regions for which Gray code embedding can not achieve minimal expansion are considered.

5.2 Three-dimensional meshes

Two of the above three direct embeddings for three-dimensional meshes have dilation two and minimal expansion. These meshes and dilation-two embeddings of two-dimensional meshes yield dilation-two embeddings of the majority of three-dimensional with the decomposition technique. For instance, a $6 \times 11 \times 7$ is a submesh of a $6 \times 12 \times 7$ mesh, which decomposed as a $3 \times 3 \times 7$ mesh and a $2 \times 4 \times 1$ mesh has a minimal-expansion dilation-two embedding. The technique in [6] does not yield a dilation-two embedding, and the decomposition into the embedding of a two-dimensional mesh and Gray code embedding of one axis does not result in minimal expansion.

Performing a dilation-two embedding of a two-dimensional mesh defined by any pair of axes, and a Gray code embedding of the third axis results in one of the relative expansions

$$\frac{\lceil \ell_1\ell_2 \rceil_2 \lceil \ell_3 \rceil_2}{\lceil \ell_1\ell_2\ell_3 \rceil_2}, \frac{\lceil \ell_2\ell_3 \rceil_2 \lceil \ell_1 \rceil_2}{\lceil \ell_1\ell_2\ell_3 \rceil_2}, \text{ or } \frac{\lceil \ell_3\ell_1 \rceil_2 \lceil \ell_2 \rceil_2}{\lceil \ell_1\ell_2\ell_3 \rceil_2}.$$

The relative expansions are either equal to one or two. Note that more than one relative expansion may be one, such as for a $5 \times 10 \times 11$ mesh, or no relative expansion may be one, such as for the $6 \times 11 \times 7$ mesh. Choosing the two axes that have the lowest values of $\ell_1/\lceil \ell_1 \rceil_2$, $\ell_2/\lceil \ell_2 \rceil_2$, and $\ell_3/\lceil \ell_3 \rceil_2$, for the two-dimensional embedding results in the smallest relative expansion. For instance, for a $5 \times 6 \times 7$ mesh, the first two axes (of length five and six respectively) should be chosen for the two-dimensional embedding.

5.3 The effectiveness of graph decomposition

Combining the three two-dimensional direct embeddings with Gray code embedding by Equation (1), yields minimal-expansion, dilation-two and congestion-two embeddings of about 70% of the two-dimensional meshes for which the (pure) Gray code embedding has an expansion > 2 [12]. The average dilation is less than for the modified line compression technique in [4].

The fraction of three-dimensional meshes, for which the decomposition technique combined with the two- and three-dimensional embedding techniques yield minimal-expansion embeddings with a dilation of at most two, is given in Figure 16. In the figure, $S_i(\varepsilon)$ is the cumulative percentage of meshes that have a relative expansion ε by applying the embedding methods with an index less than or equal to i below:

1. Apply Gray code embedding.
2. Apply the modified line compression technique [4] to any pair of axes and apply Gray code to the third axis.
3. Apply the $3 \times 3 \times 3$ or $3 \times 3 \times 7$ embedding combined with Gray code by Corollary 2.
4. For an $\ell_1 \times \ell_2 \times \ell_3$ mesh, find $\ell_2'\ell_2'' \geq \ell_2$ such that $\lceil \ell_1\ell_2' \rceil_2 \lceil \ell_2''\ell_3 \rceil_2 = \lceil \ell_1\ell_2\ell_3 \rceil_2$, Corollary 2 and [4]. The procedure is repeated for decomposing ℓ_1 and ℓ_3.

For a mesh of size less than or equal to $512 \times 512 \times 512$, the cumulated percentages grows as the sequence: 28.5%, 81.5%, 82.9%, 96.1%. Applying the method in [4] to any pair of axes, only allows about 81.5% of the meshes to achieve minimal expansion. Since the congestion

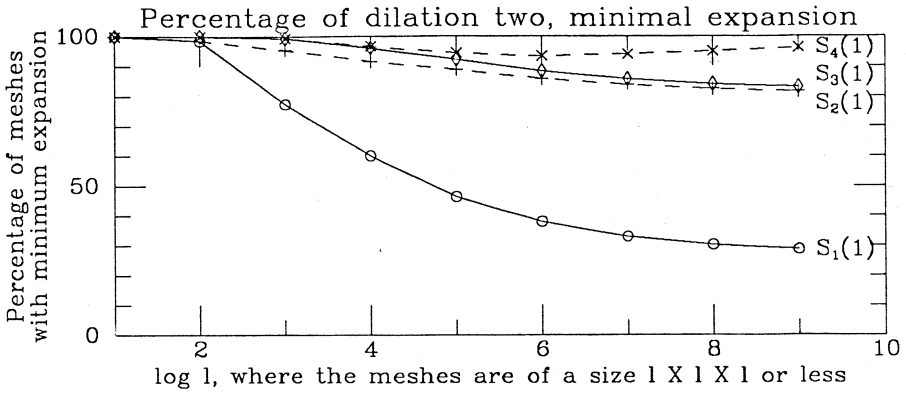

Figure 16: The cumulated percentage of the $\ell_1 \times \ell_2 \times \ell_3$ meshes where $1 \leq \ell_i \leq 2^n$ for $1 \leq n \leq 9$.

for a product graph is the maximum congestion of any graph used for the composition, any three-dimensional mesh composed from any two-dimensional mesh with a congestion two mapping, and Gray code have congestion two.

6 Embeddings of wrap-around meshes

Lemma 2 [19] *Let $\ell_i = \ell_i'\ell_i''$ and ℓ_i be even for all $1 \leq i \leq k$. Then, the $\ell_1 \times \ell_2 \times \cdots \times \ell_k$ wrap-around mesh is a subgraph of the product graph of the $\ell_1' \times \ell_2' \times \cdots \times \ell_k'$ mesh and the $\ell_1'' \times \ell_2'' \times \cdots \times \ell_k''$ mesh (both without wrap-around).*

Proof: Every $\ell_i' \times \ell_i''$ mesh for which $\ell_i'\ell_i''$ is even contains a ring of size $\ell_i'\ell_i''$ as a subgraph [19]. ∎

Let $dil_\varphi(e)$ be the dilation of the edge e under the mapping φ.

Lemma 3 *Let φ_1 be an embedding $G \rightarrow I$ and φ_2 be an embedding $I \rightarrow H$. Then, there exists an embedding function $\varphi : G \rightarrow H$ such that*

$$dil_\varphi(e) = \sum_{e_i \in \varphi_1(e)} dil_{\varphi_2}(e_i).$$

Lemma 4 *An $\ell_1 \times \ell_2 \times \cdots \times \ell_k$ wrap-around mesh M can be embedded into a minimal hypercube with dilation $\leq d + 1$, if there exists an embedding φ that maps the $\lceil \ell_1/2 \rceil \times \lceil \ell_2/2 \rceil \times \cdots \times \lceil \ell_k/2 \rceil$ mesh M_2 into a minimal hypercube with dilation d and $\lceil \prod_{i=1}^k \ell_i \rceil_2 = 2^k \lceil \prod_{i=1}^k \lceil \ell_i/2 \rceil \rceil_2$. The dilation is d, if all ℓ_i's are even.*

Proof: Consider the embedding of a $2\lceil \ell_1/2 \rceil \times 2\lceil \ell_2/2 \rceil \times \cdots \times 2\lceil \ell_k/2 \rceil$ wrap-around mesh $\tilde{M}$. By the assumptions of the lemma, Theorem 1, and Lemma 2 the wrap-around mesh $\tilde{M}$

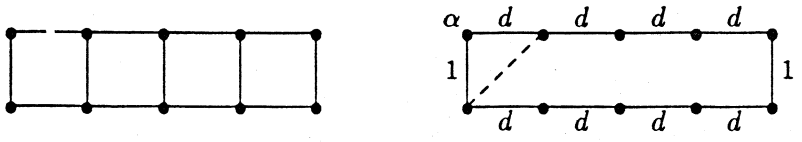

(a) (b)

Figure 17: A linear array of size ℓ_i, ℓ_i odd, embedded in the product graph of a linear array of size $\lceil \ell_i/2 \rceil$ and a 1-cube. The $\lceil \ell_i/2 \rceil$ linear array has a dilation d embedding.

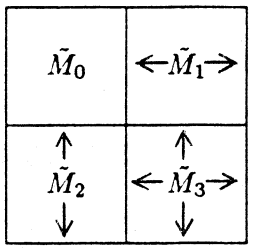

Figure 18: Partitioning for the embedding of an wrap-around mesh.

can be embedded into a minimal hypercube with dilation d. The $2 \times 2 \times 2 \cdots 2 = 2^k$ mesh is taken as the mesh M_1.

We now embed the wrap-around mesh M in the wrap-around mesh $\tilde{M}$ by removing one hyperplane for each axis i of odd length. The edge in the mesh M connecting nodes on the two sides of the removed hyperplane is simulated by a length-two path through the removed hyperplane in $\tilde{M}$. In the Boolean cube embedding of $\tilde{M}$ the removed hyperplane connects to two neighboring hyperplanes through two sets of edges of dilation one and d, respectively. The edge of M which is a path of length two in $\tilde{M}$ has a dilation of edges of $d+1$ in the cube embedding, according to Lemma 3. ∎

Figure 17-(a) demonstrates the ith coordinate of the product graph of the mesh M_2 and the k-cube for which $\lceil \ell_i/2 \rceil = 5$. All the horizontal edges have dilation $\leq d$, and all the vertical edges have dilation one. It is easy to see from Figure 17-(b) that if $\ell_i = 9$, then the node α is removed and the dilations of the two edges incident to the removed node are $\leq d$ and one, respectively. So, the dilation for the new "logical edge" (the dashed edge in the figure) is $\leq d+1$.

Intuitively, the mesh $\tilde{M}$ is partitioned into 2^k submeshes of the form $\lceil \ell_1/2 \rceil \times \lceil \ell_2/2 \rceil \times \cdots \times \lceil \ell_k/2 \rceil$. The submeshes are labeled $\tilde{M}_i$, $0 \leq i < 2^k$, such that submesh i and submesh j are adjacent if $Hamming(i,j) = 1$. Submesh $i = (i_{k-1} i_{k-2} \cdots i_0)$ is reflected for axis r if $i_r = 1$ for all r's. After this reflection the same embedding function φ is applied to all submeshes for their embeddings in their respective cubes. Figure 18 shows the four submeshes for a two-dimensional case, in which the submeshes $\tilde{M}_1$ and $\tilde{M}_3$ are reflected horizontally and the submeshes $\tilde{M}_2$ and $\tilde{M}_3$ are reflected vertically before the embedding function is applied.

Clearly, if all the ℓ_i's are even, then the condition $\lceil \prod_{i=1}^{k} \ell_i \rceil_2 = 2^k \lceil \prod_{i=1}^{k} \lceil \ell_i/2 \rceil \rceil_2$ is satisfied. If this condition holds, then the expansion remains minimal by using a mesh with

wrap-around of a slightly larger size (or of the same size) as an intermediate graph.

Lemma 5 *An $\ell_1 \times \ell_2 \times \cdots \times \ell_k$ wrap-around mesh can be embedded into a minimal hypercube with dilation* $\max(d, 2)$*, if there exists an embedding that maps the $\lceil \ell_1/4 \rceil \times \lceil \ell_2/4 \rceil \times \cdots \times \lceil \ell_k/4 \rceil$ mesh into a minimal hypercube with dilation d and $\lceil \prod_{i=1}^{k} \ell_i \rceil_2 = 4^k \lceil \prod_{i=1}^{k} \lceil \ell_i/4 \rceil \rceil_2$.*

Proof: Consider the embedding of a $4\lceil \ell_1/4 \rceil \times 4\lceil \ell_2/2 \rceil \times \cdots \times 4\lceil \ell_k/4 \rceil$ wrap-around mesh $\tilde{M}$. Apply an argument similar to the one in the proof of Lemma 4.

Figure 19-(a) and (c) shows one axis of the product graph of the mesh M_2 and the k-cube with $\lceil \ell_i/4 \rceil = 5$ and 4, respectively. All the horizontal edges have dilation $\leq d$, and all the vertical edges have dilation one. Figure 19-(b) and (d) show an embedded linear array of size $4\lceil \ell_i/4 \rceil$ (by ignoring the dashed edges). Consider the case where $\ell_i \bmod 4 \neq 0$. We wish to show that by removing one, two and three nodes, respectively, the newly formed "logical edges" have a dilation of $\leq \max(d, 2)$. When $\ell_i \bmod 4 = 1$, remove node α. When $\ell_i \bmod 4 = 2$, remove nodes β and γ (but keep node α). When $\ell_i \bmod 4 = 3$, remove all the three nodes α, β and γ. The newly-formed "logical edges" are marked by the dashed edges in the figure. Clearly, all the dashed edges preserve the property of the dilation $\leq \max(d, 2)$.

Since the above proof requires that $\lceil \ell_i/4 \rceil \geq 3$, it remains to be proved that if $\lceil \ell_i/4 \rceil = 2$ or 1, the lemma still holds. Figure 19-(e) shows for $\ell_i = 5$, 6, 7 and 8. For $1 \leq \ell_i \leq 4$, the lemma can be derived easily. ∎

Note that there exist several ways to embed a ring for Figure 19-(a) and (b) that preserve the dilation of the edges. The selected embedding minimizes the average dilation.

Corollary 3 *Any two-dimensional wrap-around mesh $\ell_1 \times \ell_2$ can be embedded into a minimal hypercube with dilation at most two, if $\lceil \ell_1 \ell_2 \rceil_2 = 16\lceil \lceil \ell_1/4 \rceil \lceil \ell_2/4 \rceil \rceil_2$ or both ℓ_1 and ℓ_2 are even. Any two-dimensional wrap-around mesh $\ell_1 \times \ell_2$ can be embedded into a minimal hypercube with dilation at most three, if $\lceil \ell_1 \ell_2 \rceil_2 = 4\lceil \lceil \ell_1/2 \rceil \lceil \ell_2/2 \rceil \rceil_2$.*

Proof: The former follows from [4], Lemmas 5 and 4. The latter follows from [4] and Lemma 4. ∎

7 Summary

A graph embedded by graph decomposition has a dilation and congestion equal to the maximum dilation and congestion of the embedding of any of the graphs into which it is decomposed. The node-congestion and active-degree of the graph is bounded from above by the sum of these quantities for each graph into which it is decomposed.

- By applying the graph decomposition technique to the mappings of 3×5, 7×9 and 11×11 meshes and Gray code embedding, 87% of the two-dimensional meshes, asymptotically, can be embedded into a minimal Boolean cube with dilation two and congestion two, and significantly lower average dilation and congestion than by the modified line compression technique [4].

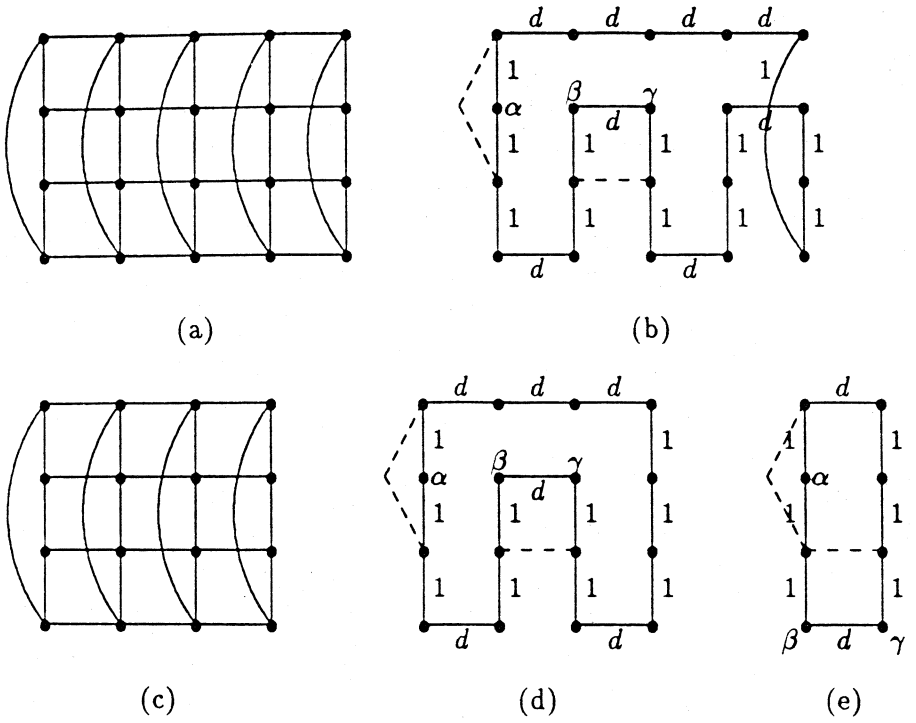

Figure 19: A linear array of size ℓ_i, embedded in the product graph of a linear array of size $\lceil \ell_i/4 \rceil$ and a 2-cube, where the latter linear array has a dilation d and the 2-cube has a dilation one embedding.

- By applying the graph decomposition technique and using the dilation-two embeddings for two-dimensional meshes [12,4] and two dilation-two embeddings of three-dimensional meshes, we have attained dilation-two minimal-expansion embeddings into Boolean cubes for 96% of all three-dimensional meshes of a size less than, or equal to, $512 \times 512 \times 512$.

The decomposition technique can be applied to the embedding of meshes with an arbitrary number of dimensions. We conjecture that a majority of the the higher dimensional meshes can be embedded with dilation two using the existing two-, and three-dimensional mesh embeddings of dilation two.

The embeddings of wrap-around meshes can be easily constructed out of the embeddings for meshes without wrap-around using the graph decomposition technique. As a special case, for all two-dimensional wrap-around meshes $\ell_1 \times \ell_2$, we have a minimal-expansion embedding with dilation two if $\lceil \ell_1 \ell_2 \rceil_2 = 16 \lceil \lceil \ell_1/4 \rceil \lceil \ell_2/4 \rceil \rceil_2$ or both ℓ_1 and ℓ_2 are even; and with dilation three if $\lceil \ell_1 \ell_2 \rceil_2 = 4 \lceil \lceil \ell_1/2 \rceil \lceil \ell_2/2 \rceil \rceil_2$ (where $\lceil x \rceil_2 = 2^{\lceil \log_2 x \rceil}$).

Acknowledgement This work has been supported in part by the Office of Naval Research under Contract N00014-86-K-0310. The authors would like to thank Quentin Stout for pointing out reference [11], Abhiram Ranade for helpful discussion of Lemma 1, and David Greenberg for his comments on a draft of this paper.

References

[1] Romas Aleliunas and Arnold L. Rosenberg. On embedding rectangular grids in square grids. *IEEE Trans. Computers*, 31(9):907–913, September 1982.

[2] Said Bettayeb, Zevi Miller, and I. Hal Sudborough. Embedding grids into hypercubes. In *Proceedings of '88 AWOC: VLSI, Algorithms and Architectures Conf.*, Springer Verlag's Lecture Notes in Computer Science, no 319, 1988.

[3] J.E. Brandenburg and D.S. Scott. *Embeddings of Communication Trees and Grids into Hypercubes.* Technical Report No. 280182-001, Intel Scientific Computers, 1985.

[4] M.Y. Chan. Dilation-2 embeddings of grids into hypercubes. In *1988 International Conf. on Parallel Processing*, The Pennsylvania State University Press, 1988.

[5] M.Y. Chan. *The Embedding of Grids into Optimal Hypercubes.* Technical Report, Computer Science Dept., University of Texas at Dallas, 1988. Appear in SPAA 89.

[6] M.Y. Chan. *Embeddings of 3-Dimensional Grids into Optimal Hypercubes.* Technical Report, Computer Science Dept., University of Texas at Dallas, 1988. To appear in the Proceedings of the Fourth Conference on Hypercubes, Concurrent Computers, and Applications, March, 1989.

[7] M.Y. Chan and F.Y.L. Chin. *On Embedding Rectangular Grids.* Technical Report TR-B2-87, Center of Computer Studies and Applications, University of Hong Kong, February 1987. to appear in IEEE Trans. Computers.

[8] Tony Chan. 1986. Personal communication.

[9] Niall Graham. *Simulations Using the Hypercube Graph.* Technical Report, Computing Research Lab., New Maxico State Univ., 1989. To appear in the Proceedings of the Fourth Conference on Hypercubes, Concurrent Computers, and Applications, March, 1989.

[10] David S. Greenberg. *Minimum Expansion Embeddings of Meshes in Hypercubes.* Technical Report YALEU/DCS/RR-535, Dept. of Computer Science, Yale Univ., New Haven, CT, August 1987.

[11] Ivan Havel and J. Móravek. B-valuations of graphs. *Czech. Math. J.*, 22:338–351, 1972.

[12] Ching-Tien Ho and S. Lennart Johnsson. On the embedding of arbitrary meshes in Boolean cubes with expansion two dilation two. In *1987 International Conf. on Parallel Processing*, pages 188–191, Penn State, 1987. Report YALEU/DCS/RR-576, April 1987.

[13] S. Lennart Johnsson. Communication efficient basic linear algebra computations on hypercube architectures. *J. Parallel Distributed Comput.*, 4(2):133–172, April 1987. (Tech. Rep. YALEU/DCS/RR-361, Yale Univ., New Haven, CT, January 1985).

[14] S. Lennart Johnsson and Peggy Li. *Solutionset for AMA/CS 146.* Technical Report 5085:DF:83, California Institute of Technology, May 1983.

[15] S. Rao Kosaraju and Mikhail J. Atallah. *Optimal Simulations between Mesh-Connected Arrays of Processors.* Technical Report, Johns Hopkins University, 1986. appear in JACM, July, 1988, page 635-650.

[16] Ten-Hwang Lai and Alan P. Sprague. *Placement of the Processors of a Hypercube.* Technical Report, Dept. of Computer and Information Science, Ohio State Univ., January 1989.

[17] Charles E. Leiserson. Area-efficient graph layouts (for VLSI). In *Proc. 21st IEEE Symp. Foundations Comput. Sci.*, pages 270–281, IEEE Computer Society, 1980.

[18] Marilynn Livingston and Quentin F. Stout. Embeddings in hypercubes. In *Proceedings Sixth International Conference on Mathematical Modelling*, pages 222–227, 1988. Preprint in August, 1987.

[19] Yuen-Wah E. Ma and Lixin Tao. Embeddings among toruses and meshes. In *1987 International Conf. on Parallel Processing*, pages 178–187, IEEE Computer Society, 1987.

[20] E M. Reingold, J Nievergelt, and N Deo. *Combinatorial Algorithms.* Prentice-Hall, Englewood Cliffs. NJ, 1977.

[21] M. Zubair and S.N. Gupta. *Embeddings on a Boolean Cube.* Technical Report, Dept. of Computer Science, Old Dominion Univ., Norfolk, Virginia, January 1989.